The membrane attack complex drives thrombotic microangiopathy in complement mediated atypical hemolytic uremic syndrome

OPEN

Kate Smith-Jackson[1,2], Patrick Walsh[1,2], Wioleta M. Zelek[3], Thomas Hoyler[4], Marianne M. Martinic[4], Gemma Thompson[1,2], Beth Gibson[1,2], Chloe Connelly[1,2], Isabel Y. Pappworth[1,2], Mark J. Murphy[4], David Kavanagh[1,2] and Kevin J. Marchbank[1,2]

[1]*Complement Therapeutics Research Group, Newcastle University Translational and Clinical Research Institute, the Medical School, Newcastle-upon-Tyne, UK;* [2]*National Renal Complement Therapeutics Centre, the Royal Victoria Infirmary, Newcastle-upon-Tyne, UK;* [3]*UK Dementia Research Institute Cardiff and Division of Infection and Immunity, School of Medicine, Cardiff University, Cardiff, Wales, UK; and* [4]*Idorsia Pharmaceuticals Ltd., Allschwil, Switzerland*

Introduction of complement (C) inhibition into clinical practice has revolutionized the treatment of patients with complement-mediated atypical hemolytic syndrome (aHUS). Our $C3^{D1115N}$ mouse model, engineered around a gain of function point mutation in C3, is associated with complement mediated aHUS in man, allowing us to study the clinical disease in a preclinical model. Backcrossing our model onto C7 deficient and C5aR1 deficient mice enabled further determination of the roles of the C5a-C5aR1 axis and C5b-9 (the membrane attack complex) on kidney disease. C7 deficiency completely abolished both clinical and histological evidence of disease. Removing *C5aR1* (CD88) attenuated the risk of developing clinical disease, but mice still developed thrombotic microangiopathy. Therapeutic inhibition strengthened our genetic findings showing both anti-C7 therapy and an oral C5aR1 antagonist, when used before evidence of significant kidney injury, prevented mice from succumbing to disease. However, there was ongoing histological disease within mice treated with the C5aR1 antagonist. Our data suggest that both C5aR1 and C7 play a role in the development of the conditions required for thrombotic microangiopathy of the kidney. While disrupting the C5a-C5aR1 axis is beneficial, our genetic and therapeutic studies showed that thrombotic microangiopathy of the kidney can still develop and ultimately our data confirm that the membrane attack complex is required to develop thrombotic microangiopathy of the kidney. Overall, our study shows that in addition to requiring alternative pathway dysregulation, local generation of membrane attack complex within the kidney is also critical to drive disease pathology in complement-mediated aHUS.

Kidney International (2025) ■, ■–■; https://doi.org/10.1016/j.kint.2024.12.016

Correspondence: *Kate Smith-Jackson, National Renal Complement Therapeutics Centre, the Royal Victoria Infirmary, Newcastle-upon-Tyne, UK. E-mail: Kate.Smith-Jackson@newcastle.ac.uk*

Received 5 December 2023; revised 18 November 2024; accepted 16 December 2024

KEYWORDS: aHUS; C3 gain-of-function; complement; MAC; therapy; TMA

Translational Statement

While loss of C5aR1 ameliorates clinical disease, C7 deficiency prevents the development of complement-mediated thrombotic microangiopathy, suggesting that preferentially targeting the terminal complement pathway at C7 could provide disease remission in patients with complement-mediated thrombotic microangiopathy, while leaving the C5a-C5aR1 axis available to aid the patient in dealing with infections.

The introduction of complement inhibition into clinical practice has revolutionized the treatment of patients with complement-mediated atypical hemolytic syndrome (aHUS); C5 inhibition reduces the incidence of end-stage renal disease and enables successful transplantation in those who have reached end-stage renal disease.[1–4] As complement therapeutics evolve, targeted agents are progressing through preclinical and clinical trials. Refining complement inhibiting therapy has the potential advantages of easier administration, reducing the immunosuppressive burden and enabling wider access to medication through reduction in costs. Successfully adopting a refined treatment approach requires a detailed understanding of the pathogenesis. In aHUS, the importance of C5a or C5b-9 in driving complement-mediated thrombotic microangiopathy (TMA, the histologic process resulting in the clinical disease) remains to be fully elucidated. Current literature is conflicting; a mouse model engineered around a complement factor H (*CFH*) mutation found no benefit of C5aR1 deficiency on renal TMA formation, whereas a model induced by antiphospholipid antibodies found the C5a-C5aR axis critical to disease development.[5,6] Thus, understanding the contributions of C5a-C5aR and C5b-9 on disease development may help

guide future treatment strategies for both existing and novel drugs that target the complement system. Given the rarity of complement-mediated aHUS coupled with the mortality and morbidity associated with treatment failure, preclinical models offer an invaluable translational insight and test bed to ascertain if there is a clinical rationale to justify change from the current gold standard of treatment. We used the $C3^{D1115N}$ mouse model of complement-mediated TMA[7] to determine the role of the C5a-C5aR1 axis and C5b-9 on disease.

METHODS

Mice

B6-$C3^{D1115N}$ mice were maintained in house and were genotyped as previously described.[7] RRID:IMSR_JAX:006845 (*C5ar1*^{tm1Cge} or Balb/c-*C5aR1*$^{-/-}$) and RRID:MMRRC_042133-MU (C57BL/6N-$C7^{em1(IMPC)J}$/J or B6-$C7^{-/-}$) were purchased from the Jackson Laboratory (JAX Lab).[8] B6-$C3^{D1115N}$ were backcrossed for 4 generations onto either the Balb/c-$C5aR1^{-/-}$ or B6-$C7^{-/-}$background. Resulting mice, heterozygous for $C3^{D1115N}$, were then intercrossed to produce the homozygous Balb/c-$C3^{D1115N}$.*C5aR1*$^{-/-}$ and B6-$C3^{D1115N}$.$C7^{-/-}$ lines, respectively. In addition, Balb/c-$C3^{D1115N}$.*C5aR1*$^{-/-}$ mice were subsequently backcrossed onto wild-type Balb/c to produce a Balb/c-$C3^{D1115N}$(.$C5aR1^{+/+}$) line. Genotyping for C5aR1 deficiency was performed by polymerase chain reaction following methods provided by the JAX lab (https://www.jax.org/Protocol?stockNumber=006845&protocolID=23815). Deletion of the C7 gene was monitored by polymerase chain reaction using primer pairs 5′-ATG°GCT°CTT°CCT°CTC°ATC°TCC-3, 5′-CTG°CAG°CTC°TCT°GAA°TGA°AAG°T-3, 30 cycles (annealing 64.8 °C), generating 415 bp (wild type) and 168 bp (C7KO). A humanized C5aR1 receptor knock-in mouse was generated by Cyagen Biosciences (under contract from Idorsia; B6.$C5aR1^{tm2(hC5aR1)Idor}$), and this was crossed onto the $C3^{D1115N}$ background for 4 generations producing $C3^{D1115N}$.$hC5aR1^{+/+}$ mice. Power calculations were used to guide N in experiments at outset based on previous survival curves or variation in complement deposition in the kidney.[7] All animal experiments were approved by the animal welfare and ethics review board of Newcastle University and the UK Home office under the auspices of animal procedure licenses PD86B3678 and PP2560803. The ARRIVE (Animal Research: Reporting In Vivo Experiments) reporting guidelines were used.[9]

C5aR1 inhibition

We tested the ability of the oral C5aR1 antagonist ACT-1014-6470[10] to protect mice from disease. Mice were placed on diet, *ad libitum* from weaning, containing ACT-1014-6470 (with estimated dosing being calculated to 45 mg/d, i.e., 20 g of mouse eating approximately 3 g of diet daily) or a matched diet without the drug for 8 weeks with daily health checks. Any mice reaching predefined clinical scores for renal disease or general welfare concerns were euthanized during the study, with the remaining culled at the end of the study where blood and tissue were harvested as described below.

Anti-C7 inhibition

Within 24 hours of weaning, $C3^{D1115N}$.$hC5aR^{+/+}$ homozygote animals were treated with either anti-C7 monoclonal antibody (mAb; 73D1 provided by Dr. W. Zelek) or $IgG_{2a,k}$ isotype control (cultured in sterile conditions in house from ECACC hybridoma 2:D12; 40 mg/kg) via intraperitoneal injections every 7 days for 8 weeks. Mice underwent daily health checks, and any mice breaching the predefined clinical scores for renal disease or general welfare were euthanized and tissues collected as above.

Mouse clinical monitoring and terminal blood analysis

Mice were monitored daily (weighing and urinalysis—Combistix; Siemens) from weaning, reducing to weekly from 2 months of age, in the absence of detectable clinical disease. Mice reaching clinical end point, as defined by welfare constraints agreed with the animal welfare and ethics review board, were euthanized and tissues harvested. Because of the restraints of clinical monitoring, blinding was not practical in these experiments. Mice that remained clinically well were culled in aged cohorts at 3, 6, and 12 months of age. Where possible, blood was collected using cardiac puncture under terminal anesthesia into precoated lithium heparin syringes (in many cases mice were found in crisis, with insufficient blood volume/hemodynamic pressure to allow blood draw during terminal cardiac puncture). Where available and possible, blood urea nitrogen (BUN) and hemoglobin (Hb) measurements were obtained using an iSTAT analyzer with a CHEM 8+ cartridge, following the manufacturer's instructions (Abbott Laboratories Ltd.).

Flow cytometry for reticulocyte and platelet count

To measure reticulocyte or platelets, 10 µl of heparinized blood was mixed with 1 ml of phosphate-buffered saline control or 1 ml of BD reticulocyte agent (BD Retic-Count; BD Biosciences) for 30 minutes at room temperature or with 400 µl of fluorescence-activated cell sorting flow buffer (phosphate-buffered saline containing 5% w/v bovine serum albumin, 1 mM ethylenediamine tetraacetic acid, 0.1% w/v Na azide, plus 1 µl purified Rat Anti-Mouse CD41 clone MWReg30; BD Biosciences) for 1 hour on ice. Platelet count was established using the method previously described.[7] Samples were immediately analyzed on a fluorescence-activated cell sorting symphony (BD Biosciences). An example of this analysis is shown in Supplementary Figure S1.

Histology analysis

Kidneys were harvested, fixed in 10% formalin, and then processed and embedded in paraffin. Sections (4 µm) were then cut, stained with periodic acid–Schiff and Martius Scarlet Blue, and imaged using an Olympus X microscope. TMA is a histologic pattern of injury with no current standardized scoring system within clinical practice to enable

quantification of injury; therefore, kidney sections were reviewed, and TMA was ascribed to be present or absent.

Immunofluorescence

Methods for C3 and C9 staining are essential as previously described,[7] with minor modification. Briefly, kidneys embedded in optimal cutting temperature were frozen on dry ice. In addition to C3 and C9, fibrinogen was also analyzed. After fixation, sections were permeabilized with Triton-X, and rabbit serum used as blocking serum for fibrinogen staining. For fibrinogen, slides were incubated with sheep antihuman fibrinogen 1:100, followed by rabbit antisheep Alexa 597 (1:200; Abcam). Slides underwent repetitive washing in phosphate-buffered saline and then imaged after being mounted in the 4′,6-diamidino-2-phenylindole mounting medium. Fluorescence images were taken at ×20 on Leica DM2000 LED using a Leica DFC7000 T camera. Densitometry analysis of glomerular complement deposition was performed using ImageJ. This is presented as mean glomerular intensity (average pixel intensity on the gray scale in this area). A minimum of 10 glomeruli were scored for each mouse.

Immunohistochemistry

For F4/80 (macrophage) and Ly6-G (neutrophil) staining, frozen sections were fixed in acetone and then blocked in 3% hydrogen peroxide. After repetitive washing, sections were blocked in 20% normal goat serum and then incubated with recombinant rabbit antimouse F4/80 (1:100; Abcam) or rat antimouse Ly6-G 9 (1:50; R&D systems), followed by goat antirabbit horseradish peroxidase (1:200; Abcam) or goat antirat horseradish peroxidase (1:200; Abcam) for Ly6-G. After further washing, sections were incubated with DAB, counterstained with Meyers hemotoxylin, and then dehydrated through graded alcohols and mounted in DPX. Images were then taken using an Olympus X microscope at original magnification ×20 and analyzed using a freely available macro plug-in for ImageJ (Immunohistochemistry Image Analysis Toolbox, open source available online).

Statistical analysis

All statistical analyses were undertaken using GraphPad prism v9.0. Mantel-Cox was used for survival analysis. For the statistical test between 2 or more groups, a test of normality (Kolmogorov-Smirnov) was undertaken, and when met, an unpaired Student's *t* test was performed. If unmet, then a Mann-Whitney test was used. Welch's correction was applied if 2 groups were not assumed to have the same SD. Two-way analysis of variance with Tukey's multiple comparison test was used to establish significance between the groups and across time. A P value of <0.05 was taken as statistically significant. P values are identified as follows: ns, nonsignificant; $^{*}P < 0.05$; $^{**}P < 0.01$; $^{***}P < 0.005$; and $^{****}P < 0.0001$. Data are shown as mean ± SEM.

RESULTS

C7 deficiency prevents renal TMA in the B6-C3^{D1115N} animal model

We have previously demonstrated that B6-C3^{D1115N} mice develop a spontaneous TMA associated with significant microangiopathic hemolytic anemia (MAHA) culminating in the death of greater than 50% of animals within the first 10 weeks of life, which could be rescued via C5 deficiency.[7] The work of the group of Song demonstrated that C6 and C9 were important for a renal TMA to develop, while disrupting C5a-C5aR1 signaling had little effect.[5] Therefore, we sought to corroborate the importance of the membrane attack complex (MAC) in our B6-C3^{D1115N} model of complement-mediated TMA through cross to a C7-deficient background. Over a period of 12 months, all 20 B6-C3^{D1115N}.C7$^{-/-}$ mice survived in contrast to a contemporaneous cohort of B6-C3^{D1115N} animals, where only 6 mice survived and only 2 of 14 mice survived TMA free (Figure 1). Postmortem histology of the kidney collected at various time points revealed no evidence of TMA in B6-C3^{D1115N}.C7$^{-/-}$ kidneys, compared with significant evidence of TMA in B6-C3^{D1115N} controls (with 4 of 6 surviving mice having evidence of TMA after histologic examination at the end point, Figure 2). The data suggest that C7 (and C5b-9) is essential for the development of a complement-mediated TMA in this model. BUN, Hb levels, and reticulocyte and platelet counts were all comparable to healthy baseline controls in the C7-deficient C3^{D1115N} animals (Figure 3) in keeping with no MAHA and the absence of TMA. Surviving B6-C3^{D1115N} with TMA (purple symbols) versus those without (blue symbols) had higher BUN on average, correlating with disease, although this was not reflected in the Hb levels. However, B6-C3^{D1115N} mice that required sacrifice (red symbols) uniformly had significantly worse kidney function and lower Hb than surviving B6-C3^{D1115N} (Figure 3). The fibrin deposition seen in TMA[5] is significantly reduced in the B6-C3^{D1115N}.C7$^{-/-}$ mice when

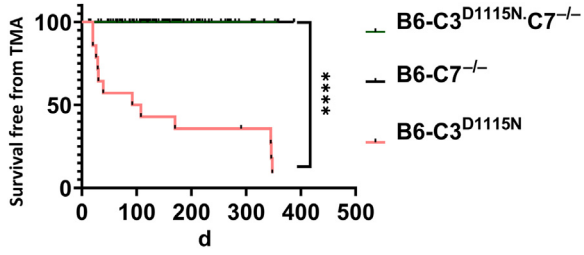

Figure 1 | One-hundred percent survival free from renal thrombotic microangiopathy (TMA) in the B6.C3^{D1115N}.C7$^{-/-}$. B6.C3^{D1115N}.C7$^{-/-}$ animals were monitored for renal disease (proteinuria/hematuria) from postpartum day 15 until they reached 3 (n = 7), 6 (n = 6), and 12 (n = 7) months of age. No animals succumbed to disease, and no TMA was detected on histologic examination, as per B6-C7$^{-/-}$ control animals at 3 (n = 3), 6 (n = 4), and 12 (n = 6) months of age. However, 8 of 14 B6.C3^{D1115N} animals succumbed to TMA during the study, and a further 4 were found to have TMA on histologic analysis at the end point (denoted by the sharp drop in "survival free from TMA" at 1 year). The Mantel-Cox test was used to establish significance. $^{****}P < 0.0001$.

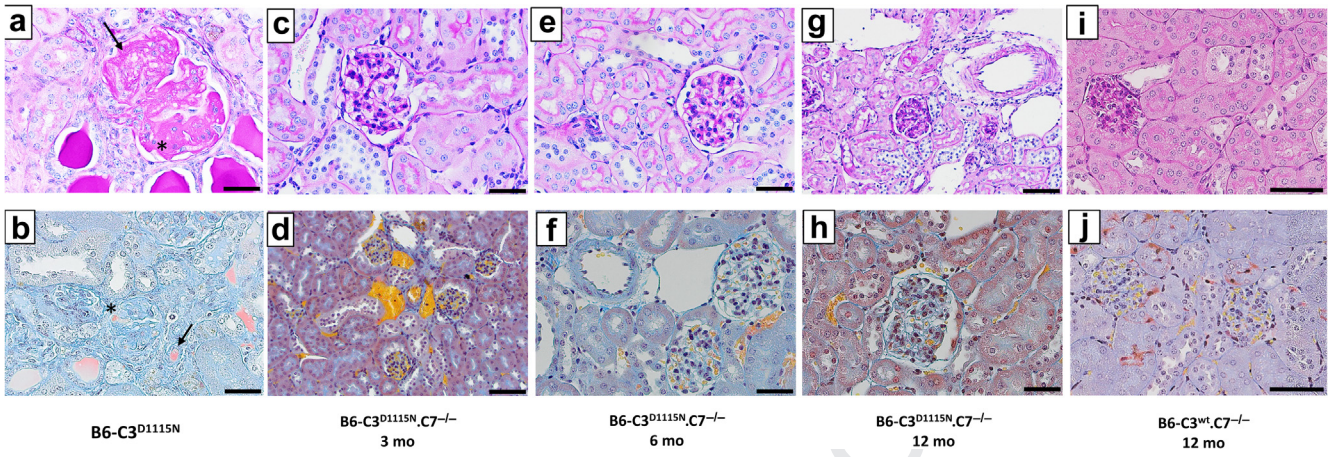

Figure 2 | C7 deficiency prevents renal thrombotic microangiopathy in the B6-C3^{D1115N} mice. Representative periodic acid–Schiff stained (**a,c,e,g**) and Martius Scarlet Blue stained sections (**b,d,f,h**) of B6-C3^{D1115N} and B6-C3^{D1115N} C7$^{-/-}$ at 3, 6, and 12 months of age. B6-C3^{D1115N} animals (approximately 2 months) (**a**) show segmental sclerosis (as indicated by *), mesangiolysis (as indicated by arrow) (**b**), and glomerular fibrin deposition (indicated by * and arrow); collectively, these are features of thrombotic microangiopathy. Normal glomeruli seen in the B6-C3^{D1115N}.C7$^{-/-}$ at 3 months (**c,d**), 6 months (**e,f**), and 12 months (**g,h**) of age. (**i,j**) Representative images of B6-C3^{WT}.C7$^{-/-}$ at 12 months of age showing normal glomeruli. Bar = 20 μm (**a–h**) and 70 μm (**i,j**). WT, wild type. To optimize viewing of this image, please see the online version of this article at www.kidney-international.org.

compared with C3^{D1115N} controls (Figure 4b, d, f, and h). However, levels of C3 glomerular deposition increase in the kidney of B6-C3^{D1115N}.C7$^{-/-}$ mice with age (Figure 4a, c, e, and g), but this is not accompanied with any evidence of MAHA, hematuria, proteinuria, or increased BUN levels (Figures 2 and 3). This finding is entirely consistent with that

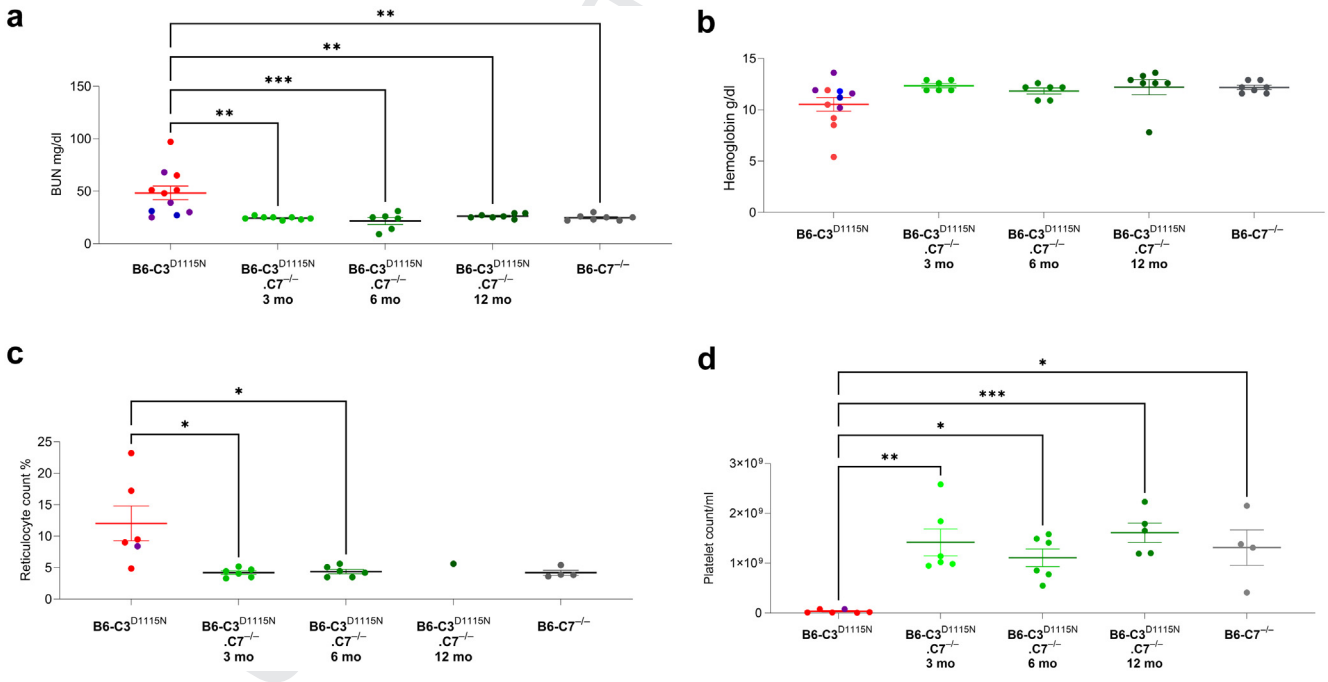

Figure 3 | C7 deficiency protects against renal injury and microangiopathic hemolytic anemia. Where available, mouse blood was analyzed via iSTAT and flow cytometry; See the Methods section. Lower blood urea nitrogen (BUN) levels and corrected hemoglobin were seen in the B6-C3^{D1115N}.C7$^{-/-}$ cohorts when compared with the B6-C3^{D1115N} controls. The control group is further subdivided by symbol color: red = culled due to health concerns in study, purple = survived to 1 year but had thrombotic microangiopathy (TMA) on histologic analysis, and blue = mice that survived and did not have evidence of TMA (**a,b**). Normalization of reticulocyte was achieved through C7$^{-/-}$ deficiency in the 3- and 6-month cohort, and data from the one available sample suggest that this remains the case at 12 months (**c**). The resolution of thrombocytopenia was observed in the B6-C3^{D1115N}.C7$^{-/-}$ when compared with the B6-C3^{D1115N} (**d**). Two-way analysis of variance with Tukey's multiple comparison test was used to establish significance between the groups of mice and across time. Only significant results between the multiple comparison are shown, with *$P < 0.05$, **$P < 0.01$, ***$P < 0.005$, and ****$P < 0.0001$. Values from individual mice are represented by dots, with mean ± SEM illustrated.

FLA 5.7.0 DTD ■ KINT4098_proof ■ 4 February 2025 ■ 11:22 pm ■ ce

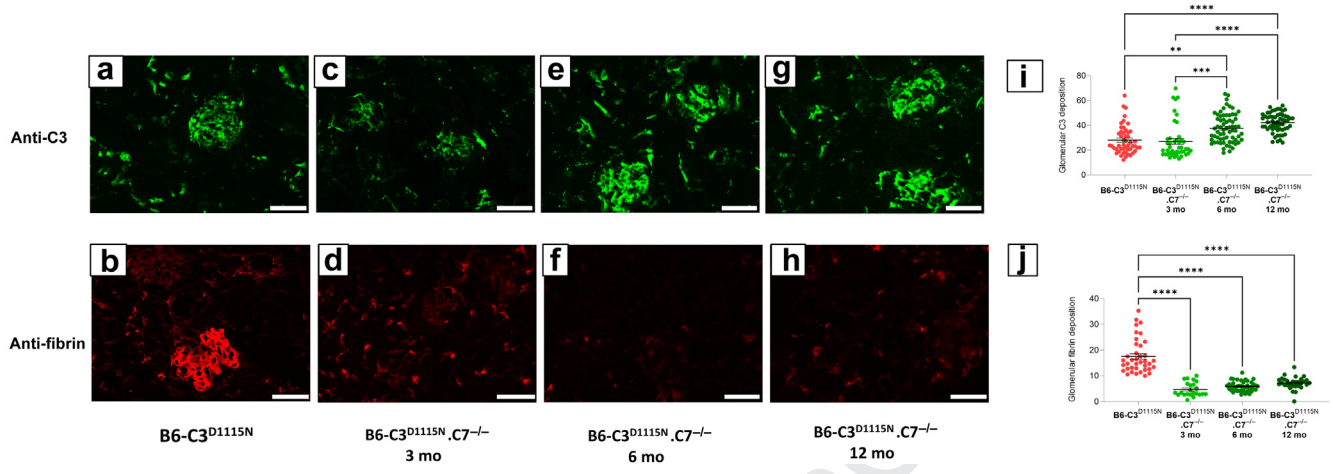

Figure 4| C7 deficiency and the glomerular complement burden in the B6.C3^{D1115N} mice. Representative immunofluorescence images of C3 (**a,c,e,g**) and fibrin (**b,d,f,h**) deposition in the B6-C3^{D1115N} and B6-C3^{D1115N}.C7$^{-/-}$ mice taken on a Leica DM200 at original magnification ×20. The exposure time was kept constant for the individual fluorophores. (**i,j**) Images were saved as LIF files and then opened as 8 BIT images in ImageJ. The region of interest (glomerulus) was demarcated, and then mean glomerular intensity for this area was calculated within the software. Bar = 50 μm. Values from individual glomeruli are represented by dots, with mean ± SEM illustrated. Two-way analysis of variance with Tukey's multiple comparison test was used to establish significance between the groups and across time. Only significant results between the multiple comparison are illustrated, with $^{**}P < 0.01$, $^{***}P < 0.005$, $^{****}P < 0.0001$. To optimize viewing of this image, please see the online version of this article at www.kidney-international.org. Q29

seen in age-matched C3^{D1115N} mice with a C5 deletion (Supplementary Figure S2). As expected, no evidence of MAC (C7 deposits, Supplementary Figure S3C) was noted in the glomerulus of these mice. However, unexpectedly, an increased expression of native C9, which may be aggregated or polymerized (see Supplementary Figure S3), was detected, but given that C9 can be detected in glomeruli of healthy 12-month-old B6.C3^{WT}.C7$^{-/-}$ mice (Supplementary Figure S3I), the increased C9 staining is not overtly pathogenic and could be a mouse phenomenon as C9 staining is decreased in kidney biopsies from patients receiving eculizumab.[11,12]

C5aR1 deficiency reduces TMA development in a Balb/c-C3^{D1115N} model

To investigate the role of the C5aR1-C5a axis in pathogenesis, we next crossed the mice to a C5aR1-deficient line on the Balb/c background (while not allowing for seamless comparison between the arms of this study, this was a choice of necessity at the time, recognizing that this is a study limitation). The Balb/c.C3^{D1115N} line that was generated as a strain-specific control demonstrated spontaneous renal TMA, with MAHA, proving that the transfer of the D1115N change in C3 to the Balb/c background would drive clinical disease irrespective of background genetic variation (see Supplementary Figure S4).

Despite Balb/c-C3^{D1115N}.C5aR1$^{-/-}$ mice showing a significant survival benefit (27 of 34 survived) versus Balb/c-C3^{D1115N} animals, 4 of 34 animals in the aging Balb/c-C3^{D1115N}.C5aR1$^{-/-}$ cohort died as a result of renal TMA (Figure 5b and c). The remaining 3 deaths had alternative causes, that is, bad teeth or litter runt; they could not be attributed to renal disease as the animals had clear urinalysis and no histologic evidence of disease. In an additional attempt to help explain the death of the remaining 3 animals, the Balb/c-C3^{D1115N}.C5aR1$^{-/-}$ underwent a further comprehensive histologic review of the brain, lung, heart, liver, spleen, and bone marrow at Charles River research animal diagnostics, but no significant pathology was identified (data not shown). Postmortem histologic analysis of the Balb/c-C3^{D1115N}.C5aR1$^{-/-}$ surviving mice (at the prescribed end point) showed that 3 of 7 mice taken at the 6-month cull and a further 3 of 5 taken in the 12-month cull showed histologic evidence of TMA (Figure 6e–h). No mice (n = 15) taken in the 3-month cull showed evidence of TMA.

Surviving Balb/c-C3^{D1115N}.C5aR1$^{-/-}$ show improved clinical parameters

In the Balb/c-C3^{D1115N}.C5aR1$^{-/-}$ mice that remained clinically well until their allotted end point, we found no biochemical evidence of an impaired renal function as determined by normal BUN levels compared with age-matched controls (Figure 7a). Furthermore, Hb levels and platelet and reticulocyte counts were within normal limits (Figure 7b–d). These results come with the caveat that in mice that succumbed to TMA and died acutely, that is, 4 of 34, no blood was available for real-time analysis of renal function or MAHA parameters, and so these results are inevitably skewed toward surviving mice. The fact that some mice with histologic evidence of TMA (Figure 6) had essentially normal levels of BUN may highlight that there has been renal recovery, and we are visualizing a historical TMA injury, which is not affecting renal excretory function at our defined end point and only becomes evidence on postmortem review. Consequently, this suggests that the removal of the C5a-C5aR1 axis can attenuate the disease process.

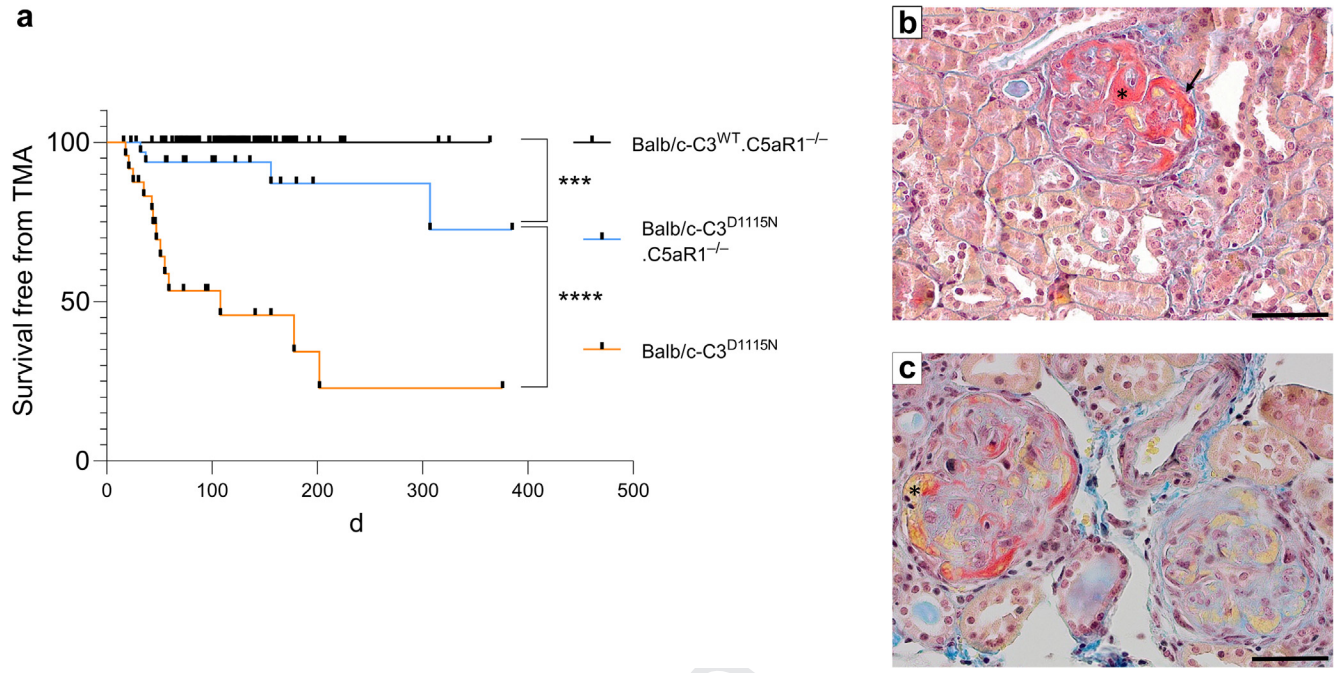

Figure 5 | Survival free from thrombotic microangiopathy (TMA) is considerably improved on the Balb/c-C3^{D1115N}.C5aR1$^{-/-}$ background. (**a**) Seven animals in the Balb/c-C3^{D1115N}.C5aR1$^{-/-}$ cohort (n = 34) were euthanized due to health concerns, and histologic evidence of TMA was identified in 4 of the animals. Of the 24 Balb/c-C3^{D1115N} mice, 13 succumbed to TMA. (**b,c**) Martius Scarlet Blue stains of 2 of the BALB/c-C3^{D1115N} mice that were culled due to health concern and found to have TMA on histologic analysis. The Mantel-Cox test was used to establish significance. ***$P < 0.005$; ****$P < 0.0001$. Bar = 50 μm. WT, wild type. To optimize viewing of this image, please see the online version of this article at www.kidney-international.org.

C5aR1 deficiency reduces C9 and fibrin in the Balb/c-C3^{D1115N} kidney

The evidence that C5aR1 deficiency attenuates the disease process is further substantiated through the significant reduction in fibrin deposits in the glomeruli of Balb/c-C3^{D1115N}.C5aR1$^{-/-}$ mice (Figure 8c, f, i, l, and o). Similar to what was observed in the B6-C3^{D1115N}.C7$^{-/-}$ mice, C3 glomerular deposits were increased in Balb/c-C3^{D1115N}.C5aR1$^{-/-}$ mice over time (Figure 8a, d, g, j, and m).

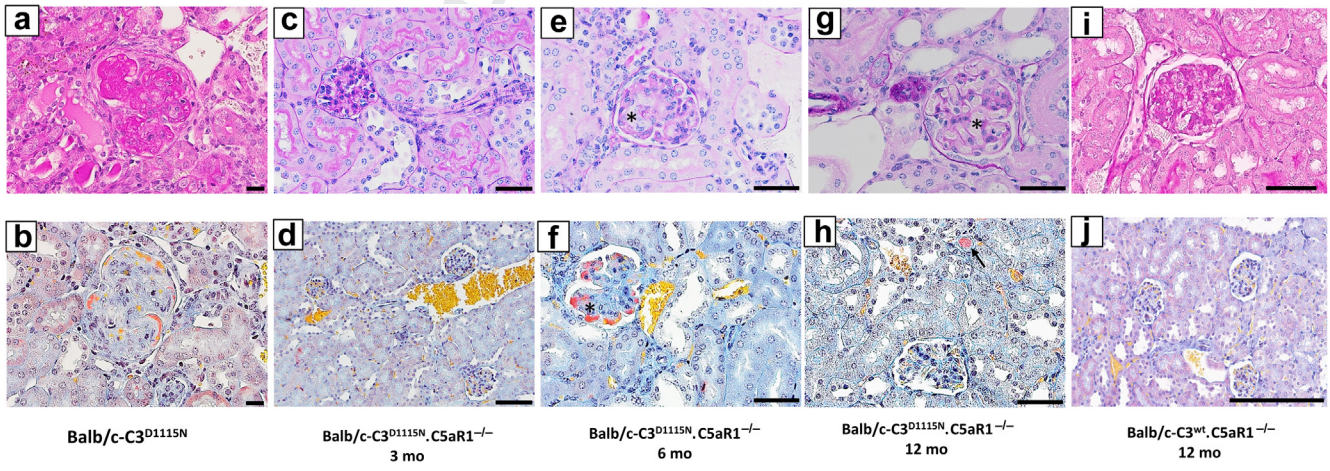

Figure 6 | Renal limited thrombotic microangiopathy (TMA) detected in aging Balb/c-C3^{D1115N}.C5aR1$^{-/-}$. Balb/c.C3^{D1115N}.C5aR1$^{-/-}$ were clinically monitored from postpartum day 15 and culled in 3- (n = 15), 6- (n = 7), and 12-month (n = 5) cohorts. (**a,b**) Representative images of Balb/c-C3^{D1115N} (2–3 months old) showing histologic features of TMA. Postmortem histologic evidence of TMA was detected in Balb/c-C3^{D1115N}.C5aR1$^{-/-}$ mice in the 6- (n = 3/7) and 12-month (n = 3/5) cohorts evidenced through periodic acid–Schiff and Martius Scarlet Blue–stained sections (**e,f,g,h**). In (**e**), * shows mesangiolysis, (**f**) * Illustrates fibrin deposition, (**g**) * shows microaneurysm formation, and (**h**) the arrow is highlighting the thrombus. (**i,j**) Representative images of Balb/c-C3^{WT}.C5aR1$^{-/-}$ at 12 months of age showing normal glomeruli. Light microscopy images were taken on the Olympus SC 50, and images were then exported as TIFF files. Bar = 10 μm (**a,b**), 20 μm (**c–i**), and 200 μm (**j**). WT, wild type. To optimize viewing of this image, please see the online version of this article at www.kidney-international.org.

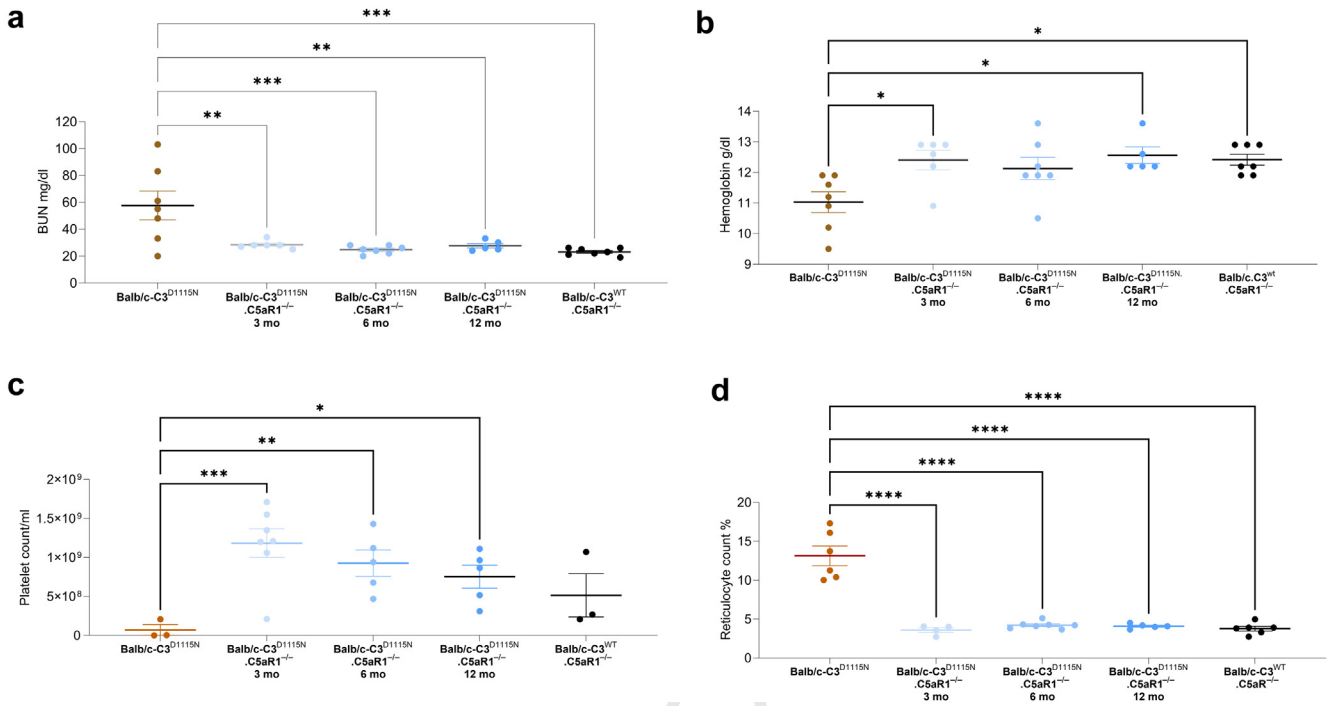

Figure 7 | Thrombotic microangiopathy (TMA) is not detectable on clinical parameters. Lower blood urea nitrogen (BUN) levels and corrected hemoglobin were seen in the Balb/c-C3^{D1115N}.C5aR1$^{-/-}$ cohorts when compared with the Balb/c-C3^{D1115N} controls (**a,b**). Resolution of thrombocytopenia was observed in Balb/c-C3^{D1115N}.C5aR1$^{-/-}$ when compared with the Balb/c-C3^{D1115N} (**c**). Normalization of reticulocyte count was achieved through C5aR1 deficiency (**d**). Insufficient blood was available from the Balb/c-C3^{D1115N}.C5aR1$^{-/-}$ that succumbed to TMA to obtain measurements in these animals. Two-way analysis of variance with Tukey's multiple comparison test was used to establish significance between the groups and across time. Only significant results between the multiple comparison are illustrated, with *$P < 0.05$, **$P < 0.01$, ***$P < 0.005$, ****$P < 0.0001$. WT, wild type.

Pharmacologic blockade of C5aR1 or C7 attenuates disease and provides a clear survival benefit

To determine whether pharmacologic blockade of C5aR1 or an anti-C7 mAb attenuates the disease process (mitigating against the strain difference of the Balb/c.C5aR$^{-/-}$ mice, thus allowing seamless comparison), we used an oral C5aR1 antagonist (ACT-1014-6470)[10] or a weekly intraperitoneal injection of an anti-C7 mAb.[13] To use the oral C5aR1 agent, which is only active on the human receptor, humanized C5aR1 mice were generated in which the mouse C5aR1 was replaced with human C5aR1. After intercross and generation of a new C3^{D1115N}.hC5aR1$^{+/+}$ double knock-in line, we carried out standard analysis to confirm that the phenotype remained unchanged in the C3^{D1115N}.hC5aR1$^{+/+}$ line. As expected, key features of a renal TMA were readily identified, validating the humanized model for therapeutic testing (Figure 9a–f).

Mice receiving the C5aR1 antagonist ACT-1014-6470 (approximately 45 mg/day) after weaning (for 8 weeks via diet) showed 100% survival compared with only 35% survival for C3^{D1115N}.hC5aR1$^{+/+}$ mice on a normal diet (Figure 9a). However, there was evidence of renal disease (25ery/ul hem for at least 2 consecutive days) in 3 mice on the oral treatment (Figure 9b) with 6 of 12 animals exhibiting postmortem histologic evidence of a TMA at the end of the study. Although there was histologic evidence of a TMA, the mice did not meet criteria necessitating euthanasia within the study duration. Indeed, only the 3 mice with renal disease detected by urine analysis showed a slight elevation in BUN levels in the treatment group (normal range: 20–36 mg/dl, Figure 9g), reflecting improved renal function across the treatment cohort. When assessing markers of MAHA, normal parameters were observed in the mice receiving the C5aR1 antagonist, except for platelet numbers, which remained low in some of the treated animals (Figure 9h–j). The slightly elevated BUN and marginally lower platelet numbers in some treated mice compared with control may reflect the fact that we also found a spectrum of histologic disease (Figure 9k–n). These findings are not surprising and mimic those seen in the Balb/c-C3^{D1115N}.C5aR1$^{-/-}$ strain where genetic knockout of C5aR1 did not prevent a TMA. Similarly, and as expected, 100% survival was achieved with anti-C7 mAb treatment compared with the isotype control (Figure 10a). One mouse was removed from the treatment study for analysis due to postmortem finding that the kidney was hydronephrotic. There was no evidence of hematuria in any other mice on anti-C7 mAb treatment. Although the isotype control conferred survival protection (Figure 10a; Supplementary Figure S5), the rate of renal injury was similar across the studies, with all mice on isotype control demonstrating significant and sustained hematuria (Figure 10b). This was mirrored on histologic analysis with 100% of the isotype

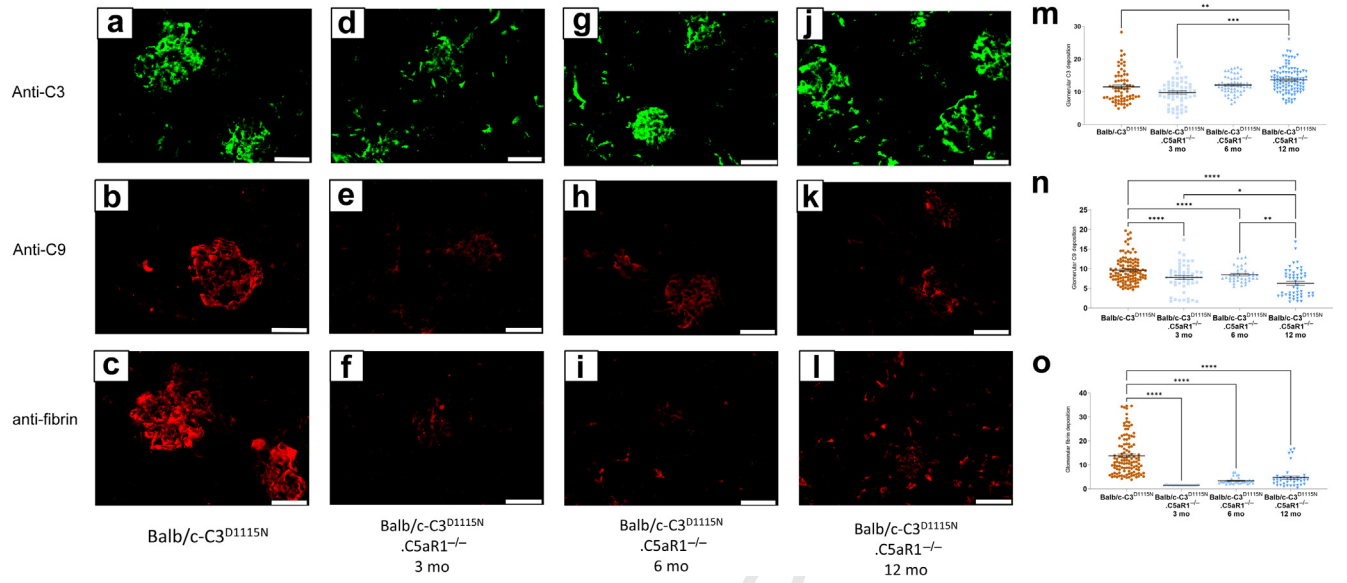

Figure 8 | Attenuation of glomerular complement deposition in the Balb/c-C3^{D1115N}.C5aR1$^{-/-}$. An initial reduction in glomerular C3 is observed in the Balb/c-C3^{D1115N}.C5aR1$^{-/-}$ 3-month cohort (**a,d,m**), with no change compared with controls at 6 months (**a,g,m**), followed by an increase in glomerular C3 deposition at 12 months of age (**a,g,m**). Glomerular C9 deposition is reduced in all aged cohorts of the Balb/c-C3^{D1115N}.C5aR1$^{-/-}$ animals (**b,e,h,k,n**). Similarly, glomerular fibrin deposition is reduced in all aged cohorts of the Balb/c.C3^{D1115N}.C5aR1$^{-/-}$ animals (**c,f,i,l,o**). A minimum number of 10 glomeruli were scored from each mouse. Immunofluorescence images were taken on the Leica DM200 at room temperature using fluorescein isothiocyanate (C3), Alexa 546 (C9), and Alexa 594 for fibrin. Bar = 50 μm (**a–i**). The exposure time was kept constant for the individual fluorophores. Images were saved as LIF files and then opened as 8 BIT images in ImageJ. Region of interest (glomerulus) was demarcated and then the mean glomerular intensity for this area calculated by the software (**m–o**). Two-way analysis of variance with Tukey's multiple comparison test was used to establish significance between the groups and across time. Only significant results between the multiple comparison are illustrated, with *$P < 0.05$, **$P < 0.01$, ***$P < 0.005$, ****$P < 0.0001$. To optimize viewing of this image, please see the online version of this article at www.kidney-international.org.

control mice showing postmortem histologic evidence of TMA, including glomeruli fibrin deposition with mesangiolysis, microaneurysm formation, and intra-arterial thrombi (Figure 10i). The anti-C7 mAb treatment resulted in lower BUN and higher Hb levels than the isotype-treated B6-C3^{D1115N}.hC5aR$^{+/+}$ (Figure 10c and e). A clear difference in the reticulocyte count was observed between the anti-C7 mAb and isotype control groups (Figure 10d). However, despite some improvement in platelet counts, these were still significantly lower than the wild-type control. Overall, anti-C7 mAb treatment improved the majority of hematological parameters. Analysis of Martius Scarlet Blue–stained sections confirmed no evidence of TMA in 7 of 8 animals treated with anti-C7 mAb (Figure 10g and h). One animal in the anti-C7 mAb therapy group was found to have glomerular sclerosis, although end point BUN was in the normal range.

Attenuation of inflammatory infiltration in the absence of C5aR1 or C7 in the C3^{D1115N} mice

Our data to date have shown that the complement-mediated TMA within the mice is initiated and driven by C5b-9, as evidenced by the complete abolishment of clinical and histologic disease in the B6-C3^{D1115N}.C7$^{-/-}$ cohorts. Renal TMA is associated with endothelial cell (EC) damage and immune cell infiltrates.[14] To investigate for the presence of neutrophils and macrophages in the kidneys of both C7- and C5aR1-deficient animals, kidneys were stained with anti-Ly6-G (neutrophils) and anti-F4/80 (macrophages; Figure 11). In C7-deficient animals, inflammatory cell infiltrates were significantly reduced compared with B6-C3^{D1115N} mice and remained equivalent to negative control animals at each time point analyzed (Figure 11a–h). We see a similar reduction in staining of F4/80 and Ly6-G when examining the Balb/c-C3^{D1115N}.C5aR1$^{-/-}$ at 6 months of age (the time point when histologic evidence of disease emerges on postmortem review; Figure 11i, i, m, n, l, and p). However, at 12 months, neutrophil infiltrate in a proportion of the Balb/c-C3^{D1115N}.C5aR1$^{-/-}$ mice is similar to that observed in Balb/c-C3^{D1115N} mice.

DISCUSSION

The C3^{D1115N} mouse model of aHUS recapitulates the clinical phenotype both on the C57BL/6[7] and Balb/c strain (Supplementary Figure S4), proving the D1115N change in C3 to be robust and reproducible in generating spontaneous complement-mediated aHUS, independent of the influence of background genetic traits in these mouse strains.[15] C7 deficiency protected C3^{D1115N} mice from developing a renal TMA and MAHA up to 12 months of age, with 0% disease penetrance compared with 85% in the B6-C3^{D1115N} mice. Therefore, we demonstrate C5b-9 to be central in initiating renal TMA *in vivo* under normal conditions and that C5a/C5aR1 amplifies the effects of C5b-9 (Figure 12). This is suggested by the observations that although *C5aR1* deficiency

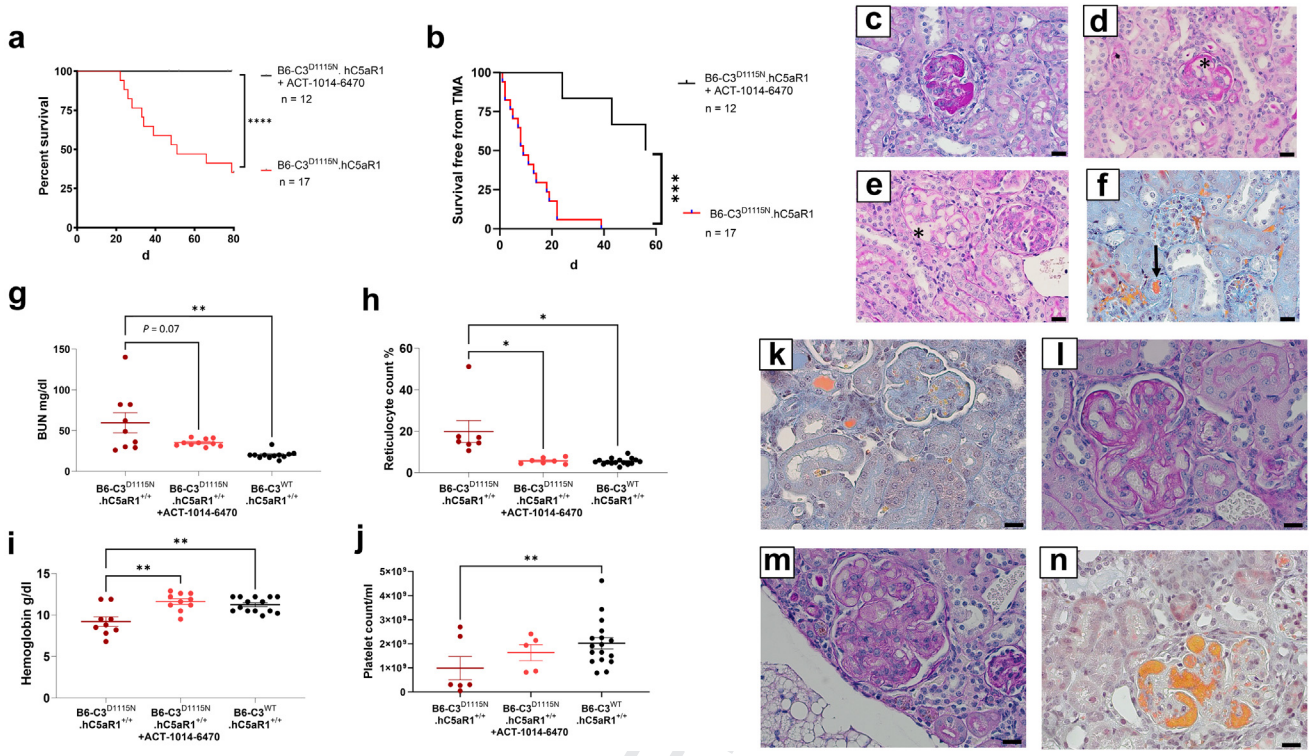

Figure 9| Oral C5aR1 inhibition in B6-C3^{D1115N}.hC5aR1$^{+/+}$ mice provides a clear survival benefit and prevents development of clinical disease. (**a**) Survival analysis shows B6-C3^{D1115N}.hC5aR1$^{+/+}$ mice succumb to a spontaneous renal thrombotic microangiopathy (TMA) in a similar fashion to the B6-C3^{D1115N} parent strain—confirming full function of the hC5aR1 knock-in gene. The data also demonstrate that early therapeutic treatment of B6-C3^{D1115N}.hC5aR1$^{+/+}$ mice with ACT-1014-6470 (C5aR1 inhibitor) via diet is highly effective. (**b**) Oral hC5aR1 antagonism does not completely prevent renal disease in the mice, that is, for at least 2 consecutive days, 25ery/ul of hematuria was detected in 3 mice, an indication of renal TMA, and an additional 3 mice were found to have renal TMA on histologic analysis after cull. Mantel-Cox was used to establish significance. (**c–e**) Periodic acid–Schiff–stained sections showing histologic features of TMA (*including double contouring and mesangiolysis) of C3^{D1115N}.hC5aR1 confirming the phenotype after the introduction of the hC5aR1. (**f**) Martius Scarlet Blue stain showing fibrin clot in a vessel in the C3^{D1115N}.hC5aR1$^{+/+}$ mouse. N = 4 examined Bar = 10 μm (**c–f**). (**g**) Blood urea nitrogen (BUN; plasma marker of kidney impairment) levels collected during terminal bleeds at the end of the study. (**h**) Mice receiving the C5aR inhibitor have higher levels of hemoglobin than untreated controls. (**i**) Reduced reticulocytosis in treated mice. (**j**) Improved platelet counts in treated mice. Two-way analysis of variance was used for statistical analysis in Graphpad. Data are shown as mean ± SEM. Only significant results between the multiple comparison are illustrated, *$P < 0.05$, **$P < 0.01$, ***$P < 0.005$, ****$P < 0.0001$. Note that as around 50% of B6.C3^{D1115N}.hC5aR$^{+/+}$ died before we were able to collect blood, the data in (**f**) thru (**i**) are skewed to surviving mice; indeed 2 mice show little or no evidence of disease at the end point. (**k–n**) Histologic analysis of C3^{D1115N}.hC5aR1$^{+/+}$ after 8 weeks of C5aR1 antagonist containing diet. Stained sections showing varied histology in the mice that received the C5aR1 inhibitor treatment; TMA was identified in 6 of 12 mice treated with a range of TMA, that is, (**k**) thrombi, (**l**) mesangiolysis/double contouring, (**m**) mesangiolysis, and (**n**) fibrin deposits. Bar = 10 μm (**k–n**). To optimize viewing of this image, please see the online version of this article at www.kidney-international.org.

(removal of the C5a-C5aR axis) clearly attenuates disease, it does not totally abolish TMA. Despite the subtle reduction in the penetrance of histologic disease observed in the Balbc-C3^{D1115N} (75% compared with 85% in the B6-C3^{D1115N} strain), which had no effect on overall mortality from TMA, we still identified histologic disease in a proportion of the Balbc-C3^{D1115N}.C5aR$^{-/-}$. Pharmacologic inhibition on the B6 background through either a C5aR1 antagonist or anti-C7 mAb further substantiated our genetic findings, particularly when suppression of renal disease (measured by active urinary sediment and histologic injury) is also accounted for. The data herein also suggest that MAC-driven inflammation is recruiting neutrophils in the absence of C5aR1 signaling, and this, over time, may contribute to TMA. We propose that while C5b-9 initiates disease, C5a-mediated signaling amplifies these igniting effects, culminating in a positive feedforward loop, with potentiated complement activation and EC activation. By removing C5a signaling through the absence of C5aR1, there is a reduction in complement-induced inflammation, reducing inflammatory infiltrate, which translates into an attenuated disease process within the kidney (Figure 12).

Our findings share some similarities with a previously published mouse model of renal TMA, a factor-H point mutation (W1206R, FH$^{R/R}$).[5] In this model, C6 and C9 deficiency significantly improved survival and diminished renal TMA, suggesting that C5b-9 contributed significantly to renal TMA. However, we did not see any significant proteinuria (beyond control levels) in the aging B6.C3^{D1115N}.C7$^{-/-}$ mice, suggesting that despite increasing

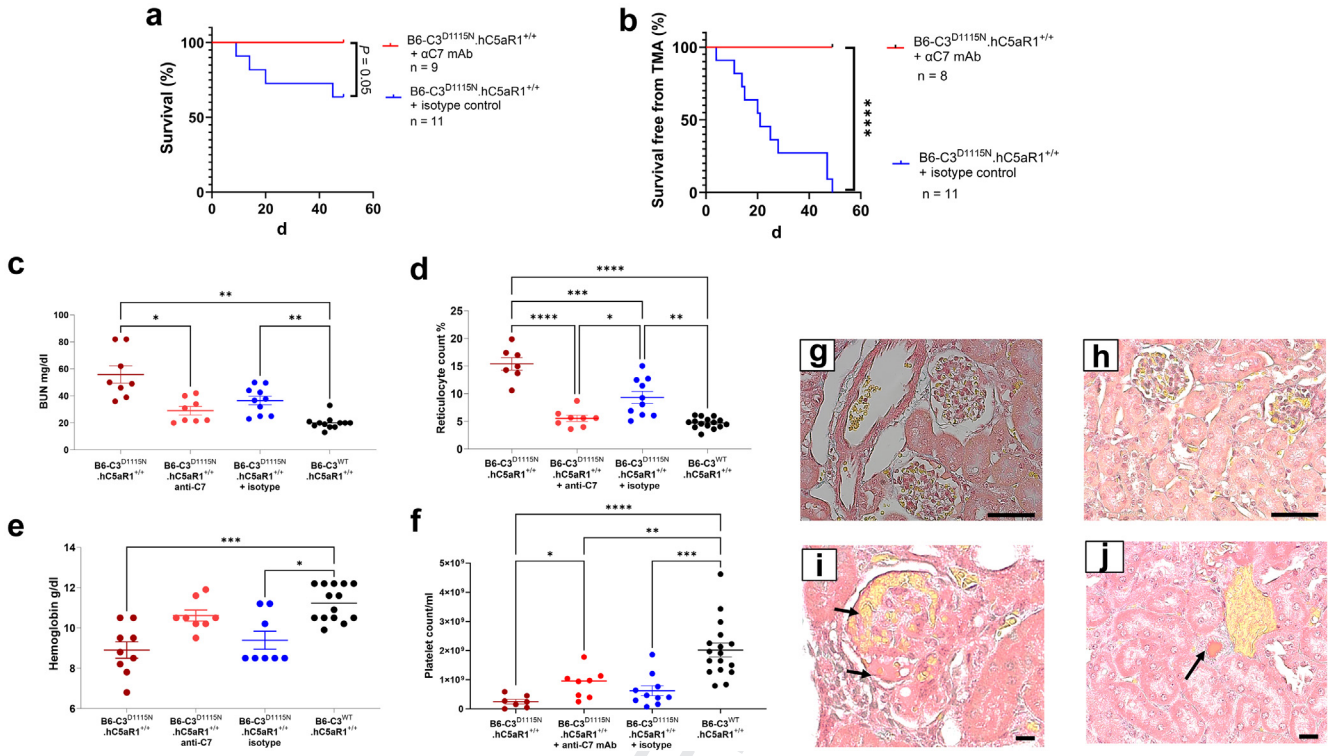

Figure 10 | Prophylactic use of an anti-C7 mAb ameliorates disease in B6-C3^{D1115N}.hC5aR1$^{+/+}$ mice. (**a**) Prophylactic treatment of B6-C3^{D1115N}.hC5aR1$^{+/+}$ mice with anti-(α)C7[13] via weekly i.p. injection from weaning confers 100% protection from disease. The isotype control is also protective (see Supplementary Figure S4), although (**b**) does not completely prevent renal thrombotic microangiopathy (TMA; 2 or more consecutive days of 25ery/ul hematuria) in the mice. Mantel-Cox was used to establish significance. (**c**) Blood urea nitrogen (BUN) levels collected during terminal bleeds at the end of the study. (**d**) Reduced reticulocytosis in treated mice. (**e**) Hemoglobin levels in treated animals are not significantly different to wild-type (WT) mice. (**f**) Improved platelet counts in treated mice. (**c,d,f**) Two-way analysis of variance with Welch's correction or (**e**) Kruskal-Wallis was used for statistical analysis using Graphpad. Data are shown as mean ± SEM. Only significant results between the multiple comparison are illustrated, $^{*}P < 0.05$, $^{**}P < 0.01$, $^{***}P < 0.005$, $^{****}P < 0.0001$. Note that one anti-C7 mAb treated B6.C3^{D1115N}.hC5aR$^{+/+}$ was removed from analysis in (**b**)–(**f**) due to a hydronephrotic kidney, and one isotype control mouse was found dead. (**g–j**) Histologic analysis of C3^{D1115N}.hC5aR1$^{+/+}$ after 8 weeks of anti-C7 monoclonal antibody (mAb) therapy. No evidence of TMA in 7 of 8 animals treated with αC7 treatment using Martius Scarlet Blue staining; representative glomeruli from 2 different mice treated with the αC7 mAb are shown with normal glomeruli (**g,h**). Bar = 20 μm (**g,h**). All isotype control mice showed histologic evidence of ongoing TMA including glomeruli fibrin deposition with mesangiolysis and microaneurysm formation (**i**) as well as an intra-arterial thrombi (**j**). Bar = 10 μm (**I,j**). To optimize viewing of this image, please see the online version of this article at www.kidney-international.org.

levels of deposited C3, this was tolerated, which was not the case in the C6-deficient FH$^{R/R}$ mouse. Furthermore, the Song group found no survival benefit with C5aR1 gene deficiency in the FH$^{R/R}$ model, and that the renal TMA persisted.[5] In addition to this, neither C6 and C9 nor C5aR1 deficiency rescued the hemolytic anemia or resolved the thrombocytopenia (although there were a variety of levels across mice). In both C3^{D1115N} and FH$^{R/R}$ mice, there is markedly reduced complement regulation by FH at cell surfaces; consequently, there is significant consumption of C3 (to 25% vs. 50% of normal levels, respectively) and C5 (to 33% vs. 52% of normal levels, respectively),[5,7] but it is important to highlight the significant difference in the FH$^{R/R}$ model to our C3^{D1115N} model. The FH$^{R/R}$ mice develop widespread macrovascular thromboses in multiple organs, which is not typical of the clinical syndrome in man, and this may link to "noncanonical or noncomplement" roles that FH is reported to play in coagulation[16] and in cell activation (via competition with FHR proteins[17]) that could be more significantly disrupted by a loss-of-function FH molecule. Interestingly, although C5aR1 deficiency rescued the macrovascular thromboses, it did not resolve thrombocytopenia in FH$^{R/R}$ mice, which in all likelihood reflects MAC-driven TMA in the kidney. The hemolytic anemia in the C3^{D1115N} mice is rescued through *C7* and *C5aR1* deficiency reflecting the restoration of health to the glomerular endothelium. The protective effects of *C5aR1* deficiency on the glomerular endothelium in C3^{D1115N} mice mirror that seen in an alternative immune complex mouse model of TMA induced by antiphospholipid antibodies where deficiency improved pathologic and clinical features of disease. *C5aR1* deficiency undoubtedly protects C3^{D1115N} mice from renal TMA in a manner akin to the APL model. Another modifier we were unable to explore is the role of the C5L2 receptor. The specific role of this receptor remains controversial, but C5adesArg (less potent form of C5a) retains high affinity to it, so may exert some effects.[18] The C3a-C3aR axis can be both inflammatory and anti-inflammatory in renal tissue depending on the context of the injury,[19] and with the

FLA 5.7.0 DTD ■ KINT4098_proof ■ 4 February 2025 ■ 11:22 pm ■ ce

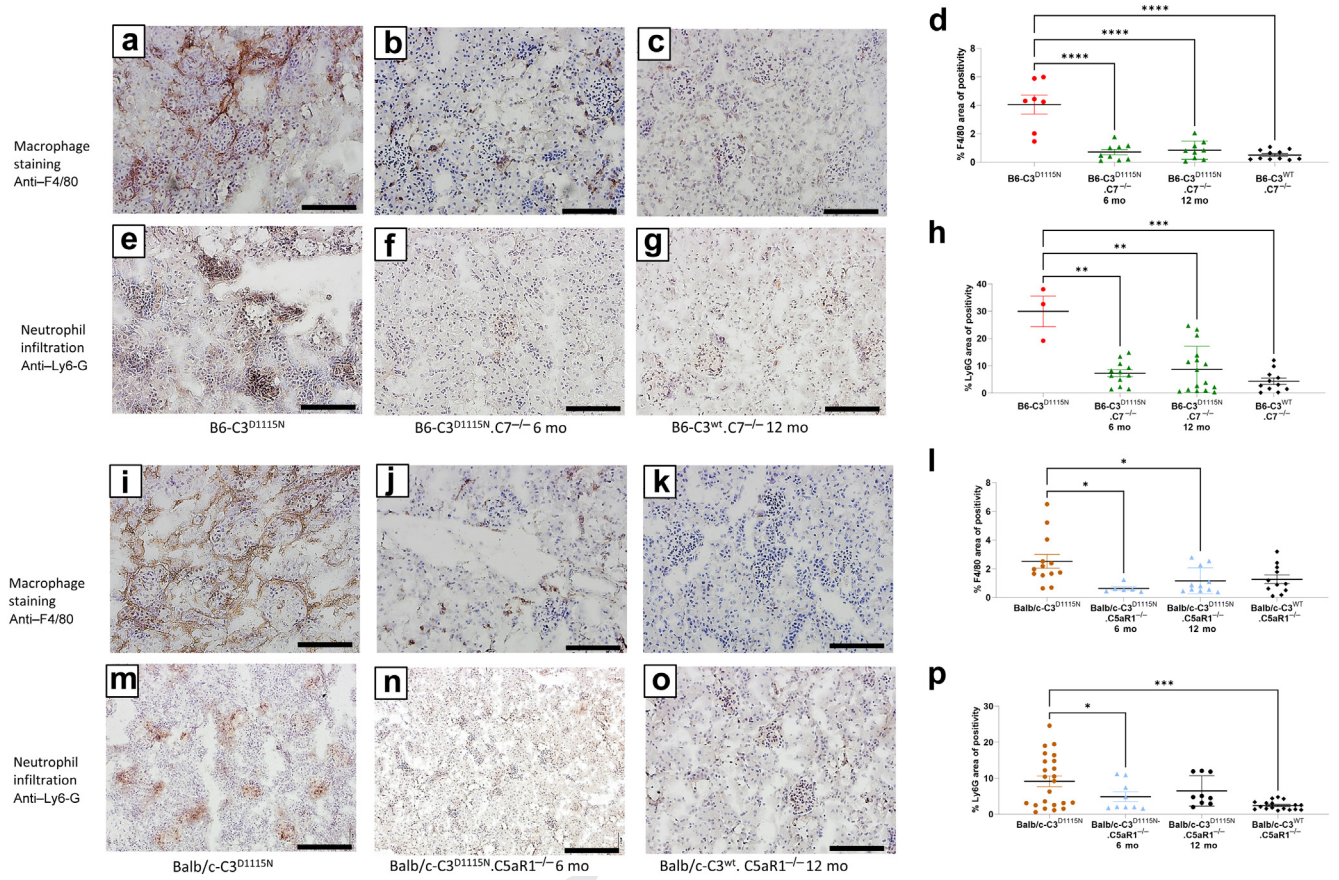

Figure 11 | Attenuation of inflammatory infiltration in the absence of C5a or C7 in the C3^{D1115N} mice. Positive F4/80 and Ly6-G staining is seen in both the B6-C3^{D1115N} (**a,e**) and Balb/c-C3^{D1115N} (**i,m**) mice. Reduced F4/80 and Ly6-G staining is seen in both the B6-C3^{D1115N}.C7$^{-/-}$ (**b,f**) and the Balb/c-C3^{D1115N}.C5aR1$^{-/-}$ at 6 months (**j,n**) or 12 months, with the exception of neutrophils in the Balb/c-C3^{D1115N}.C5aR1$^{-/-}$ mice (**o,p**), where some mice showed similar infiltrate to the Balb/c-C3^{D1115N} mice. No difference in staining was noted when deficient mice were compared with their wild-type (WT) controls—B6-C3^{WT}.C7$^{-/-}$ (**d,h**) and Balb/c-C3^{WT}.C5aR1$^{-/-}$ (**l,p**). Light microscopy images were taken on the Olympus SC 50 and were then exported as TIFF files. Bar = 200 μm (**a–g,i–o**). Two-way analysis of variance with Tukey's multiple comparison test was used to establish significance between the groups and across time. Only significant results between the multiple comparison are illustrated, with *P <0.05, **P < 0.01, ***P < 0.005, ****P < 0.0001. To optimize viewing of this image, please see the online version of this article at www.kidney-international.org.

potential increased C3 deposition in the C5aR1-deficient mice, this may also provide some additional signaling that was not as pronounced in the FH$^{R/R}$ mice and is protective in our model. These changes may in sum provide an explanation for the difference between the FH$^{R/R}$ and C3^{D1115N} models with respect to the effectiveness of deficient C5aR1 signaling in slowing disease progression.

Our genetic data demonstrate that while blockade of C7 prevents a TMA, a C5aR1 antagonist may ameliorate disease; this is clearly the case in C3^{D1115N}.hC5aR1$^{+/+}$ mice receiving the C5aR1 antagonist orally from weaning. There was no statistical difference in BUN, Hb, reticulocytes, and platelets, that is, no evidence of an MAHA was detected between the treated and wild-type control (Figure 9g–j), mirroring the protective effects of the *C5aR1* deficiency in younger mice. However, despite the survival advantage conferred by C5aR1 inhibition (i.e., 100% survival while on the drug), the pathologic features of TMA could still be readily seen in 50% of mice on treatment. We have previously demonstrated in this model that some mice develop early features of TMA by day 7 postpartum,[7] and in this study, mice could only be treated from weaning (postpartum days 21–24). Thus, some of the features seen in these mice could be due to subclinical damage before treatment; however, the development of TMA in the genetic knockout of C5aR1 indicates that blockade at this level is insufficient to prevent TMA. That ACT-1014-6470 treatment mirrored the effects of genetic knockdown of C5aR1 suggests effective target engagement, albeit in a model dependent on the MAC with only a minor amplifying effect of C5a after disease initiation. Consequently, genetic deletion of C7 in this model and that of C6 and C9 in the FH$^{R/R}$ model[5] indicate that targeting MAC is superior to targeting C5aR1. Pharmacologic inhibition with anti-C7 mAb consolidated this hypothesis and provides translational evidence that pharmacologic inhibition of C7 may prove to be a more efficacious treatment for disease remission in man, given that there was a greater level of renal injury (evidenced through an active urinary sediment and

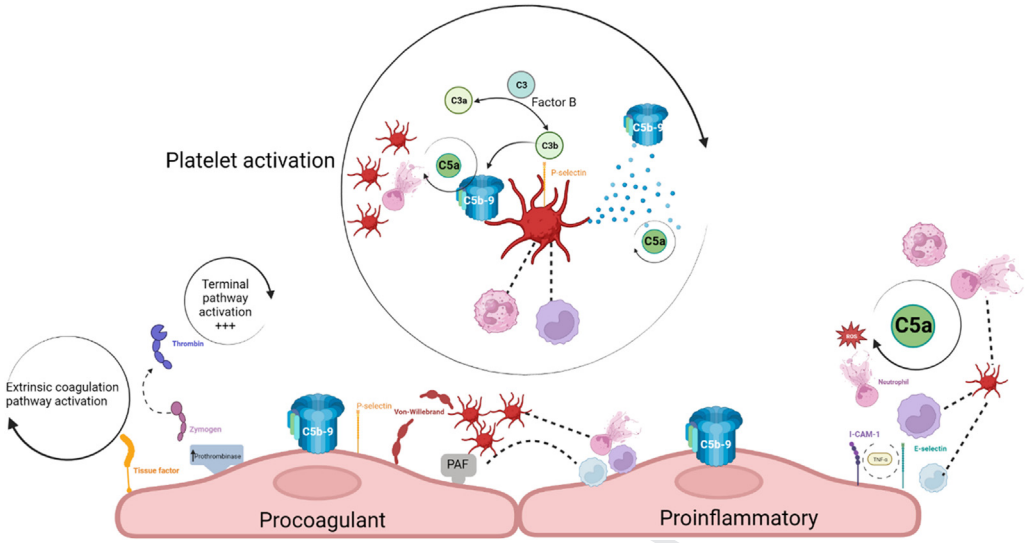

Figure 12 | Proposed mechanisms for C5b-9-driven thrombotic microangiopathy (TMA). C5b-9 ignites a series of events that lead to the activation of the endothelial cells and platelets culminating in the pathologic process of TMA. C5a amplifies the effects of C5b-9 leading to a feedforward mechanism of ongoing complement activation, endothelial cell activation, and platelet activation and aggregation. C5b-9 leads to the endothelial expression of tissue factor that activates the extrinsic pathway. An increase in prothrombinase activity leads to the increased generation of thrombin that can then independently cleave C5, leading to further terminal pathway activation. Exocytosis of P-selectin and von Willebrand factor (vWF) factor onto the endothelial cell surface leads to platelet activation and captures circulating vWF, creating an adhesive scaffold on the endothelial cell surface. Expression of platelet activating factor transforms resting platelets to activated platelets, which then leads to platelet leucocyte aggregates. Expression of intercellular adhesion molecule-1 and E-selectin in unison with tumor necrosis factor alpha (TNF-α) recruits inflammatory cells, which C5a then amplifies, leading to additional activated neutrophils. C5b-9 leads to p-selectin translocation onto the platelet surface, which provides a surface for ongoing AP activity and the release of C3, FB, and properdin, which then provides a further source for ongoing complement activation. The release of prothrombotic microparticles, C5a and C5b-9 release from platelets then amplifies the ongoing vicious cycle. All these events culminate in activated platelets encountering a primed prothrombotic endothelial cell surface, resulting in a TMA. AP, XXX; PAF, XXX.

histologic evidence of disease) on oral C5aR1 blockade compared with anti-C7 mAb.

Notably, isotype control also had a therapeutic effect (Supplementary Figure S5), possibly a mixture of plasma expansion and mild complement depletion, and inhibition of monocytes and macrophage activation, correlating with the previously described protective effects of intravenous immunoglobulin.[20] However, histologic evidence of a TMA was identified in all mice receiving the isotype control.

From current literature, it is difficult to tease apart the specific individual roles of C5b-9 and C5a on glomerular EC activation, given their individual capability to induce a prothrombotic environment.[21] C5a and C5b-9 can alter the thrombotic phenotype of the glomerular EC, triggering exocytosis of von Willebrand factor and p-selectin from Weibel-Palade bodies;[22,23] this activates the coagulation system through stimulating an increase in expression of tissue factor, which supports formation of the prothombinase complex, further potentiating platelet aggregation and modifying vascular tone.[24,25] Further, C5b-9 induces expression of adhesion molecules and platelet activation factor,[26] and C5a appears to reduce endothelial expression of thrombomodulin, increase vessel permeability, and induce platelet-leucocyte aggregates.[22] In addition to EC dysfunction, complement activation can also activate platelets. Activated platelets are, in turn, a source of complement. C5b-9 acts as a platelet agonist, releasing procoagulant particles and von Willebrand factor with simultaneous translocation of p-selectin to the platelet surface.[27–29] C5a potentiates the activation of platelets. This activated platelet surface provides a scaffold for the initiation of the alternative pathway, which is further enhanced when properdin becomes bound.[30] An alteration in the thrombotic phenotype of the EC coupled with activated platelets creates a hypercoaguable endothelial luminal environment, providing optimum conditions for a continuing renal TMA (see Figure 12).

Removing C7 prevents the activation of EC from C5b-9, thus attenuating glomerular EC activation from hyperfunctional C3 in the $C3^{D1115N}$ model of TMA. Binding of C7 to C5b6 forms a stable trimeric complex allowing it to become associated with the cell membrane.[24] The addition of C8 to C5b-7 forms a tetrameric complex that promotes binding and polymerization of C9, enabling it to induce its cytolytic activity on the cell. Both clusterin and protein S preferentially bind C7 to regulate C5b-9. Clusterin prevents the insertion of C5b-7 into the cell membrane, whereas protein S binds to C5b-7, inhibiting polymerization of C9.[24] The lytic and sublytic effects on ECs require the complex to insert into the membrane to signal the cell; thus by preventing insertion through C7 deficiency the effects are thwarted. C7 is the central portion of C5b-9 and is an important limiting factor;[31] the success of C7 deletion in abolishing disease within

our mouse model makes C7 an attractive therapeutic target. Current C5 inhibition requires continuous intravenous therapy, with a high target concentration; thus large drug doses are required to achieve a therapeutic effect.[32] Targeting C7 could circumvent this while also enabling C5a to function in its physiological roles.

Limitations

There is an obvious limitation when comparing 2 different strains of mice, that is, B6.C3^{D1115N} and the Balb/c C3^{D1115N}, which was due to the available strains of mice, that is, difficulties transporting mice during the COVID-19 pandemic. However, we believe that the therapeutic inhibition of targeting both C7 and C5aR1 on the same genetic background (i.e., B6-C3^{D1115N}.hC5aR$^{+/+}$) substantiates our genetic data. There is a smaller limitation in that the anti-C7 mAb study was conducted after the completion of the C5aR1 antagonist study rather than contemporaneously due to operation constraints, and it is possible that genetic or environmental modifiers may have changed between the studies despite mice being maintained in a heterozygous C3$^{+/N}$ background and in the same facility. Another intrinsic limitation is that fully reflective hematological analysis is dependent on mice being euthanized in a controlled manner at end point rather than succumbing to disease when researchers were not on site, and therefore, at certain points in the study, due to inaccessibility to the facilities (during the COVID pandemic), opportunities to collect the samples, as we had hoped, were not afforded to us. This will skew certain readouts toward normal when they would be expected to be more severely affected and limited the scope of analysis in certain cohorts.

In summary, the C3^{D1115N} mouse model of aHUS faithfully recapitulates the clinical manifestations of complement-mediated aHUS. Examination of *C7* and *C5aR1* deficiency over 12 months demonstrates that while loss of either is protective, there is a clear added survival benefit with C7 deficiency across time, that is, MAC is essential for the generation of TMA, while C5aR signaling provides a potentiating effect.

The data suggest that C5b-9 in the kidney plays an essential role as the trigger and driver of pathogenesis on activating the complement system in the context of complement-mediated aHUS.

This work offers key insights into disease mechanisms and as to future pharmacologic targets in complement-mediated aHUS. Future preclinical work will be required to establish if therapeutic inhibition at more advanced stages of disease (where hematuria and proteinuria are established) will induce remission in mice before clinical trials.

DISCLOSURE

KJM has received research funding from Gemini Therapeutics, Idorsia Pharmaceuticals Ltd., and Catalyst Biosciences as well as consultancy income from Freeline Therapeutics, Bath ASU, Mosaic, and MPM Capital. He also currently has a collaboration agreement with Purespring. DK was academic founder of Gyroscope Therapeutics Ltd., now a Novartis Company, and has received consultancy income and equity from Gyroscope Therapeutics Ltd. He has received honoraria for consultancy work from Alexion, Novartis, Sarepta, Silence Therapeutics, Samsung, Amgen, Chemocentryx, Apellis, and Idorsia. His spouse works for GSK. KJM and DK are authors of patent applications including recombinant complement factor I production and/or formation of the C3b/FH/FI trimolecular complex. TH, MMM, and MJM are employed by Idorsia Pharmaceuticals Ltd. and have shares.

DATA STATEMENT

All data are presented in the article. There are no genetic, proteomic, or transcriptomic data, and no specific codes or algorithms are used in this article.

ACKNOWLEDGMENTS

We thank the staff and technicians at Newcastle comparative biology centre and flow cytometry facilities for the help in conducting this study. We also thank Prof. C. Harris for helpful discussion throughout this study and Prof. B.P. Morgan and Dr. W. Zelek for providing the anti-C9 antibodies.

FUNDING INFORMATION

This study was funded by several grants from the Northern Counties Kidney Research Fund (KJM, HD, IP, GT, and CC) and the Newcastle Healthcare Charites (KJM, KS-J, and HD). KS-J is an MRC clinical fellow (MR/R001359/1). Idorsia provided funding for studies with the oral C5aR1 inhibitor and provided the humanized C5aR1 mice free of charge.

AUTHOR CONTRIBUTIONS

KJM and KS-J conceived, carried out, wrote, edited, and funded the study. PW developed the reticulocyte and platelet count assays and assisted with data collection. IP, GT, CC, and BG collected data and edited the manuscript. WMZ provided the anti-C7 mAb and edited the manuscript. TH, MMM, and MJM provided C5aR antagonist and hC5aR animals and edited the manuscript. DK provided supervision, critical analysis, and edited the manuscript.

Supplementary material is available online at www.kidney-international.org.

REFERENCES

1. Legendre CM, Licht C, Muus P, et al. Terminal complement inhibitor eculizumab in atypical hemolytic-uremic syndrome. *N Engl J Med*. 2013;368:2169–2181.
2. Rondeau E, Scully M, Ariceta G, et al. The long-acting C5 inhibitor, ravulizumab, is effective and safe in adult patients with atypical hemolytic uremic syndrome naive to complement inhibitor treatment. *Kidney Int*. 2020;97:1287–1296.
3. Glover EK, Smith-Jackson K, Brocklebank V, et al. Assessing the impact of prophylactic eculizumab on renal graft survival in atypical hemolytic uremic syndrome. *Transplantation*. 2023;107:994–1003.
4. Brocklebank V, Walsh PR, Smith-Jackson K, et al. Atypical hemolytic uremic syndrome in the era of terminal complement inhibition: an observational cohort study. *Blood*. 2023;142:1371–1386.
5. Ueda Y, Miwa T, Ito D, et al. Differential contribution of C5aR and C5b-9 pathways to renal thrombic microangiopathy and macrovascular thrombosis in mice carrying an atypical hemolytic syndrome-related factor H mutation. *Kidney Int*. 2019;96:67–79.
6. Seshan SV, Franzke CW, Redecha P, et al. Role of tissue factor in a mouse model of thrombotic microangiopathy induced by antiphospholipid antibodies. *Blood*. 2009;114:1675–1683.
7. Smith-Jackson K, Yang Y, Denton H, et al. Hyperfunctional complement C3 promotes C5-dependent atypical hemolytic uremic syndrome in mice. *J Clin Invest*. 2019;129:1061–1075.
8. Hopken UE, Lu B, Gerard NP, Gerard C. The C5a chemoattractant receptor mediates mucosal defence to infection. *Nature*. 1996;383:86–89.

9. Percie du Sert N, Ahluwalia A, Alam S, et al. Reporting animal research: explanation and elaboration for the ARRIVE guidelines 2.0. *PLoS Biol*. 2020;18:e3000411.
10. Ort M, Dingemanse J, Hsin CH, et al. First-in-human study with ACT-1014-6470, a novel oral complement factor 5a receptor 1 (C5aR1) antagonist, supported by pharmacokinetic predictions from animals to patients. *Basic Clin Pharmacol Toxicol*. 2022;131:114–128.
11. Locke JE, Magro CM, Singer AL, et al. The use of antibody to complement protein C5 for salvage treatment of severe antibody-mediated rejection. *Am J Transplant*. 2009;9:231–235.
12. Pickering MC, Ismajli M, Condon MB, et al. Eculizumab as rescue therapy in severe resistant lupus nephritis. *Rheumatology*. 2015;54:2286–2288.
13. Zelek WM, Morgan BP. Monoclonal antibodies capable of inhibiting complement downstream of C5 in multiple species. *Front Immunol*. 2020;11:612402.
14. Genest DS, Patriquin CJ, Licht C, et al. Renal thrombotic microangiopathy: a review. *Am J Kidney Dis*. 2023;81:591–605.
15. Rabe M, Schaefer F. Non-transgenic mouse models of kidney disease. *Nephron*. 2016;133:53–61.
16. Heurich M, McCluskey G. Complement and coagulation crosstalk—factor H in the spotlight. *Immunobiology*. 2023;228:152707.
17. Kopp A, Hebecker M, Svobodová E, Józsi M. Factor H: a complement regulator in health and disease, and a mediator of cellular interactions. *Biomolecules*. 2012;2:46–75.
18. Scola AM, Higginbottom A, Partridge LJ, et al. The role of the N-terminal domain of the complement fragment receptor C5L2 in ligand binding. *J Biol Chem*. 2007;282:3664–3671.
19. Gao S, Cui Z, Zhao MH. The complement C3a and C3a receptor pathway in kidney diseases. *Front Immunol*. 2020;11:1875.
20. Jefferson JA, Suga SI, Kim YG, et al. Intravenous immunoglobulin protects against experimental thrombotic microangiopathy. *Kidney Int*. 2001;60:1018–1025.
21. Schmidt CQ, Schrezenmeier H, Kavanagh D. Complement and the prothrombotic state. *Blood*. 2022;139:1954–1972.
22. Noris M, Remuzzi G. Terminal complement effectors in atypical hemolytic uremic syndrome: C5a, C5b-9, or a bit of both? *Kidney Int*. 2019;96:13–15.
23. Noris M, Galbusera M. The complement alternative pathway and hemostasis. *Immunol Rev*. 2023;313:139–161.
24. Woodruff TM, Nandakumar KS, Tedesco F. Inhibiting the C5-C5a receptor axis. *Mol Immunol*. 2011;48:1631–1642.
25. Ikeda K, Nagasawa K, Horiuchi T, et al. C5a induces tissue factor activity on endothelial cells. *Thromb Haemost*. 1997;77:394–398.
26. Hamilton KK, Hattori R, Esmon CT, Sims PJ. Complement proteins C5b-9 induce vesiculation of the endothelial plasma membrane and expose catalytic surface for assembly of the prothrombinase enzyme complex. *J Biol Chem*. 1990;265:3809–3814.
27. Polley MJ, Nachman RL. Human platelet activation by C3a and C3a des-arg. *J Exp Med*. 1983;158:603–615.
28. Polley MJ, Nachman R. The human complement system in thrombin-mediated platelet function. *J Exp Med*. 1978;147:1713–1726.
29. Hattori R, Hamilton KK, McEver RP, Sims PJ. Complement proteins C5b-9 induce secretion of high molecular weight multimers of endothelial von Willebrand factor and translocation of granule membrane protein GMP-140 to the cell surface. *J Biol Chem*. 1989;264:9053–9060.
30. Saggu G, Cortes C, Emch HN, et al. Identification of a novel mode of complement activation on stimulated platelets mediated by properdin and C3(H2O). *J Immunol*. 2013;190:6457–6467.
31. Wurzner R. Modulation of complement membrane attack by local C7 synthesis. *Clin Exp Immunol*. 2000;121:8–10.
32. Lekova E, Zelek WM, Gower D, et al. Discovery of functionally distinct anti-C7 monoclonal antibodies and stratification of anti-nicotinic AChR positive Myasthenia Gravis patients. *Front Immunol*. 2022;13:968206.